SCIENCE AND TECHNOLOGY ORGANIZATION
CENTRE FOR MARITIME RESEARCH AND EXPERIMENTATION

Reprint Series **CMRE-PR-2019-128**

Distributed underwater glider network with consensus Kalman filter for environmental field estimation

Raffaele Grasso, Paolo Braca, Stefano Fortunati, Fulvio Gini, Maria S. Greco

June 2019

Originally published in:

OCEANS 2015, 18-21 May 2015, Genoa, Italy,
doi: 10.1109/OCEANS-Genova.2015.7271659

About CMRE

The Centre for Maritime Research and Experimentation (CMRE) is a world-class NATO scientific research and experimentation facility located in La Spezia, Italy.

The CMRE was established by the North Atlantic Council on 1 July 2012 as part of the NATO Science & Technology Organization. The CMRE and its predecessors have served NATO for over 50 years as the SACLANT Anti-Submarine Warfare Centre, SACLANT Undersea Research Centre, NATO Undersea Research Centre (NURC) and now as part of the Science & Technology Organization.

CMRE conducts state-of-the-art scientific research and experimentation ranging from concept development to prototype demonstration in an operational environment and has produced leaders in ocean science, modelling and simulation, acoustics and other disciplines, as well as producing critical results and understanding that have been built into the operational concepts of NATO and the nations.

CMRE conducts hands-on scientific and engineering research for the direct benefit of its NATO Customers. It operates two research vessels that enable science and technology solutions to be explored and exploited at sea. The largest of these vessels, the NRV Alliance, is a global class vessel that is acoustically extremely quiet.

CMRE is a leading example of enabling nations to work more effectively and efficiently together by prioritizing national needs, focusing on research and technology challenges, both in and out of the maritime environment, through the collective Power of its world-class scientists, engineers, and specialized laboratories in collaboration with the many partners in and out of the scientific domain.

NOTE: The CMRE Reprint series reprints papers and articles published by CMRE authors in the open literature as an effort to widely disseminate CMRE products. Users are encouraged to cite the original article where possible.

Distributed Underwater Glider Network with Consensus Kalman Filter for Environmental Field Estimation

Raffaele Grasso[*], Paolo Braca[*]
[*]Research Department, STO Centre for Maritime Research and Experimentation, (STO-CMRE)
Viale San Bartolomeo 400, 19126 La Spezia, Italy
{Raffaele.Grasso, Paolo.Braca}@cmre.nato.int

Stefano Fortunati[#§], Fulvio Gini[#§], Maria S. Greco[#§]
[#]Dept. of Information Engineering, University of Pisa, Italy
[§]CNIT RaSS (Radar and Surveillance System) National Laboratory, Pisa, Italy
{stefano.fortunati,m.greco,f.gini}@iet.unipi.it

***Abstract*—A distributed coordinated dynamic sensor network for optimal environmental field estimation is proposed and tested on simulated and real data. The architecture is used to distribute the estimation of 3D time-varying fields on a network of underwater gliders in which communication constraints are one of the main limiting factors for achieving complete network automation and de-centralization. The dynamic network is integrated with a network of relay nodes that the agents can reach at the surface through satellite or radio links. Local field statistics are estimated by a Kalman filter-based algorithm by agents and the information in the network is shared by using the asynchronous consensus algorithm. The system is tested on realistic scenarios that are simulated by true oceanographic forecast models. A heterogeneous network of underwater and surface wave gliders is used to estimate 3D sea water temperature fields. Simulation results show that the network achieves a consensus with an average root mean square error at steady state that is below 0.5 °C.**

Keywords—autonomous vehicles; distributed processing; sensor networks; consensus; optimal field esimation.

I. Introduction

The autonomous capability of robotic sampling networks, able to satisfy in real time prescribed requirements, allows high quality ocean field estimation and forecast [1]. At the same time, managing and automatic control of such networks is challenging. These issues can be tackled by the recent advances in distributed statistical signal processing techniques related to the control and the inference in dynamic sensor networks [2][3][4][5][6][7][8]. This work proposes a networked processing and control strategy for optimally estimating environmental spatial fields in a distributed fashion by a fleet of autonomous underwater vehicles (agents) in which communications among agents are not possible. The agents sporadically emerge to perform satellite or radio communications to communicate with one (or more) relay nodes (RN). The RN acts as an information gateway to asynchronously diffuse the local information collected by a sensor to all the sensors. The global estimation of the spatial field is, in this way, iteratively computed and somehow shared by all the nodes of the network. The estimation algorithm is based on the decomposition of the field in a series of spatial radial basis functions with unknown coefficients [2][8]. The coefficients are estimated by using measurements locally collected by agents. Each agent estimates the coefficient vector and covariance by the Kalman filter. The local estimates are exchanged with the other nodes through a RN. In particular, this latter forms a local coefficient estimate (with the related covariance) by combining the local estimates of the agents, when available, through the consensus algorithm [4][5]. The agents also apply the consensus with RNs in order to update their local estimates. The information is diffused among the network by asynchronously exchanging coefficient estimates and associated covariance, providing, at steady state regime, a global estimate of the field distributed among all the nodes of the network (including the RNs). Each agent optimizes its trajectory by using the estimate of the field error in order to acquire field measurements in the most informative areas and adaptively track the field variations.

This work is based on previous work presented in [9] and [10] by the authors. In this contribution, the network scenario is heterogeneous (see Fig. 1). The purpose of the study is to integrate different autonomous vehicles, both at surface and underwater, and fixed surface buoys. In particular, the case with underwater gliders and wave surface gliders is considered, with a network of fully connected fixed buoys acting as an information exchanging network of RNs with limited communication ranges.

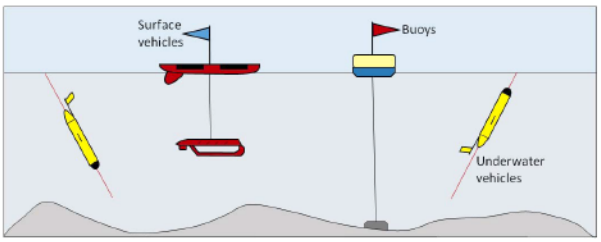

Fig. 1. Heterogenous sensor network scenario.

All the nodes in the network communicate by line-of-sight radio links. The RN network can be also integrated with a node achievable through a satellite link which can be exploited by an agent (wave glider or underwater glider when at surface) if an RN at surface is not in the line-of-sight. A further

scenario, not considered here, sees underwater gliders exchanging information with wave gliders in the line-of-sight, thus integrating the fixed RN network with a dynamic one. Moreover, the study assumes that acoustic underwater communications are not possible between agents and between agents and RNs that is a practical case as the vehicles here considered are usually not equipped with a long range acoustic communication transmitter/receiver. Nevertheless, the simulation framework here proposed allows the integration of such capabilities in an easy way and the effects of short range acoustic links will be investigated in future work.

The distributed estimation and dynamic sensor network control algorithm proposed in this work has several advantages. The nodes asynchronously exchange locally updated estimates of the field coefficient vector and the associated covariance. In principle, the measurement model of a network node can be unknown to the other agents so that different sampling devices, for instance, can be allowed in the same network (see for example [9] for the case of agents equipped with compressive sensing devices [11]). Furthermore, the agents have not to exchange their positions with other agents and RNs, and the control of an agent is local, based on its present position and its local field coefficient and covariance estimates that converge to the global ones thanks to the consensus algorithm. Compared to a solution in which the agents exchange their measurements with the RN nodes and the control is centralized, the approach here followed makes the integration of new agents in the network very easy and the control of an agent robust to communication failures with the RN network. On the contrary, the information exchange overhead is increased by the two-way transmission of the coefficient covariance matrix whose size should be limited by carefully choosing the number of base functions in the field expansion. Future work will be devoted to counteract this issue by limiting the information transfer to a reasonable level.

The proposed system is tested on a realistic simulated scenario making use of a 3D time varying temperature field from the Navy Coastal Ocean Model (NCOM) forecast model [12] over the area of interest of the Recognized Environmental Picture 2011 (REP11) experiment in Mediterranean Sea, Italy, organized and conducted by the Science and Technology Centre for Maritime Research and Experimentation (STO–CMRE). The tests show the feasibility of the proposed system in terms of field variability tracking and estimation error at regime, achieving average root mean square error within 0.5 °C.

The paper is organized as follows. Section 2 describes the system architecture. In particular the field model, the agent sequential estimation algorithm, the consensus algorithm and the agent control law will be detailed. Section 3 reports the results of the simulation on the REP11 scenario while section 4 ends the paper with conclusions and future work.

II. SYTEM DESCRIPTION

The proposed sensor network is based on an expansion of the scalar field on a basis of given functions and on dynamic agents that estimate the expansion coefficients sequentially by a Kalman filter. The global field estimation is achieved by exchanging local estimates with the RNs and combining them by a consensus fusion algorithm. The agents use estimated covariance to control the position of the next measurement toward areas of higher uncertainty. The next subsections will describe each component in detail.

A. *Field model*

This section and the next provide an overview of the local field estimation algorithm performed by each sensor. The estimation procedure relies on the expansion of the spatial field on a basis of known spatial functions, weighted by unknown coefficients, which are in general time variant. The spatial field to be estimated can be written as [2]:

$$g(\mathbf{r},t) = \mathbf{\Psi}(\mathbf{r})^T \mathbf{c}(t) = \sum_{j=1}^{L} c_j(t)\psi_j(\mathbf{r}) , \quad (1)$$

where $\mathbf{r}$ is the coordinate vector of the 2D or 3D region of interest, t is the time variable, $\mathbf{c}(t)=[c_1(t),\ldots,c_L(t)]^T$ is the (possibly time-varying) real coefficient vector and $\mathbf{\Psi}(\mathbf{r})=[\psi_1(\mathbf{r}),\ldots, \psi_L(\mathbf{r})]^T$ is the vector of the base functions that depends only on the position vector $\mathbf{r}$. Given the base vector $\mathbf{\Psi}(\mathbf{r})$, the problem of estimating the scalar field $g(\mathbf{r},t)$ is equivalent to estimate the coefficient vector $\mathbf{c}(t)$. In this work, we assume that the coefficient vector is constant or slowly time-varying. The base functions in (1) are assumed to be of the radial type. In particular, a set of Gaussian-like radial basis functions (RBF), $\psi_j(\mathbf{r})=\exp(-\|\mathbf{r}-\mathbf{r}_j\|^2/\beta)$, is chosen with a given spread parameter β (constant for all the functions) and centers $\mathbf{r}_j$ located on a regular grid in the spatial region of interest.

B. *Kalman filter sequential estimation*

The agent local sequential estimation of the field is performed by a Kalman filter in which the coefficient dynamic is modeled by a linear state space equation shared by all the agents in the network:

$$\mathbf{c}_{i,k} = \mathbf{F}_k \mathbf{c}_{i,k-1} + \mathbf{n}_{i,k} , \quad (2)$$

where $\mathbf{F}_k$ is a known state transition matrix, $\mathbf{n}_k$ is a Gaussian distributed independent noise vector with covariance matrix $\mathbf{Q}_{i,k} = \mathrm{diag}(\sigma^2_{1,i,k},\ldots,\sigma^2_{L,i,k})$. The identity matrix is usually used in the case the transition matrix is unknown [13]. In this case, the matrix $\mathbf{Q}_{i,k}$ can be considered as a free parameter that can be tuned to adjust the velocity at which the system adapts its estimate to the true dynamic of the coefficients [13]. The tradeoff to be considered is between filtering response of the system and estimate residual error [13].

Assuming a network composed of N sensors, the i^{th} sensor, for $i=1,\ldots,N$, acquires at each time step a noisy measurement $y_{i,k}$ of the field. According to (1), the measurement equation of the i^{th} sensor can be expressed as follows:

$$y_{i,k} = \mathbf{\Psi}(\mathbf{p}_{i,k})^T \mathbf{c}_{i,k} + e_{i,k} , \quad (3)$$

where $\mathbf{\Psi}(\mathbf{p}_{i,k})$ is the vector of the spatial base function evaluated at the position vector $\mathbf{p}_{i,k}$ of the i^{th} sensor at time step k, $e_{i,k}$ is the scalar Gaussian measurement noise, independent from $\mathbf{n}_{i,k}$, with zero-mean and variance $\rho^2_{i,k}$. Each sensor runs

the Kalman filter prediction and update steps to provide the sequential estimate of the coefficient vector $\hat{\mathbf{c}}_{i,k}$ and its covariance matrix $\hat{\mathbf{C}}_{i,k}$ to an RN.

C. Heterogenoeus sensor network integration protocol

This section describes how local estimates from each network agent can be exploited to achieve global field estimation in a distributed fashion. The architecture has to cope with the underwater agents communicating sporadically with the RNs network once at surface. The resulting network has a switching topology [14] and is based on the consensus paradigm [15][16]in which the information is diffused among the agents through the relay nodes, which essentially act as an information gateway (see Fig. 2).

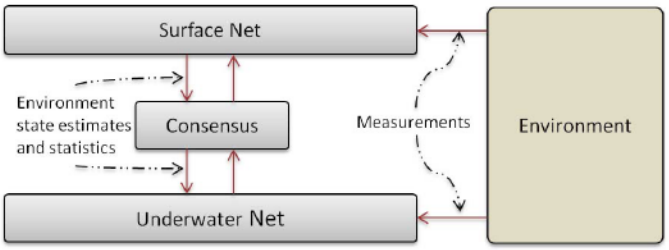

Fig. 2. Integration of hetereogenoes sensor network through consensus.

In the proposed network model, agents can communicate with a relay node (RN) at random instants but cannot communicate among each other. Each agent sequentially estimates the coefficient vector by means of a KF from local field measurements and updates its position applying a control law and using the local prediction of the coefficient estimate covariance matrix. Agents communicating with the RNs transmit their local coefficient vector estimate and covariance; no field measurements are provided to RNs. RNs distribute their estimate (coefficient vector and covariance) to the connected agents and update their estimates by combining the local agent's estimates, when available, through the average consensus algorithm [4][5], or propagates the previous estimate if no agents are connected. Agents connected to RNs update their local estimates by using RN estimates through average consensus.

The protocol allows the global information to "intermittently flow" into the network through relay nodes with a collaborative behavior among the agents who emerge above the sea surface to start the communication. Realistic numerical simulations show that all local agent estimates and RN estimates statistically converge close to the true global coefficient vector *i.e.* the network reaches a consensus.

D. Consensus algorithm

The network of agents and relay nodes are modeled as an undirected graph with the topology in Fig. 3. The whole network has a set of $N+N_r$ nodes, $\mathrm{N}=\{1,2,\ldots,N+N_r\}$, with $\{N,\ldots, N+N_r\}$ being the indices of the relay nodes, and an adjacency matrix given by:

$$\mathbf{A}=\begin{bmatrix}\mathbf{I}_{N\times N} & \mathbf{1}_{N\times N_r}\\ \mathbf{1}^T_{N\times N_r} & \mathbf{1}_{N_r\times N_r}\end{bmatrix} \tag{4}$$

which defines the set of all possible graph edges $\varepsilon=\{(i,l)|A_{i,j}=1, i,l\in\mathrm{N}\}$ ($\mathbf{I}_{N\times N}$ is the $N\times N$ identity matrix, while $\mathbf{1}_{N\times N_r}$ and $\mathbf{1}_{N_r\times N_r}$ are the $N\times N_r$ and $N_r\times N_r$ matrix of all ones, respectively).

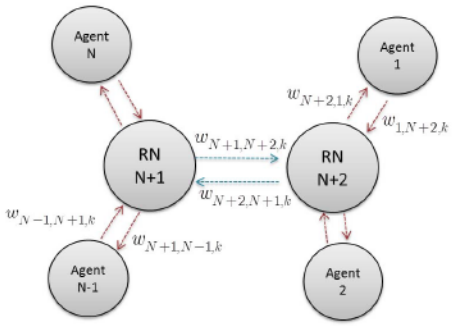

Fig. 3. Star network topology with time varying link weights.

Actually, the structure of the network is dynamic *i.e.* at each time step k, there is a subset $\varepsilon_k\subseteq\varepsilon$ of edges which are active, where an edge $i,l\in\varepsilon_k$ is active if node i can communicate with node l. At each k, the consensus algorithm is applied to the local estimates of the information matrices, $\hat{\mathbf{D}}_{i,k}=\hat{\mathbf{C}}^{-1}_{i,k}$, and the information vectors, $\hat{\mathbf{g}}_{i,k}=\hat{\mathbf{D}}_{i,k}\hat{\mathbf{c}}_{i,k}$, at each node, included the relay node(s):

$$\begin{aligned}\hat{\mathbf{g}}_{i,k+1}&=\sum_{l\in\mathrm{N}_{i,k}} w_{i,l,k}\hat{\mathbf{g}}_{l,k}\\ \hat{\mathbf{D}}_{i,k+1}&=\sum_{l\in\mathrm{N}_{i,k}} w_{i,l,k}\hat{\mathbf{D}}_{l,k}\end{aligned}, \tag{5}$$

where $\mathrm{N}_{i,k}$ is the set of node neighbors of the i^{th} node (the node i is included in the set) at time step k and $w_{i,l,k}$ are weighting parameters. Once the consensus has been applied, the updated coefficient estimate and the associated covariance for the i^{th} node are $\hat{\mathbf{c}}_{i,k+1}=\hat{\mathbf{D}}^{-1}_{i,k+1}\hat{\mathbf{g}}_{i,k+1}$ and $\hat{\mathbf{C}}_{i,k+1}=\hat{\mathbf{D}}^{-1}_{i,k+1}$, respectively. The choice of the weights in the consensus update is crucial for guaranteeing certain properties and asymptotic convergence. In particular, in this work, the Metropolis weights are considered:

$$w_{i,l,k}=\begin{cases}1/\left[1+\max(d_{i,k},d_{l,k})\right] & (i,l)\in\varepsilon_k\\ 1-\sum_{l\in\mathrm{N}_{i,k}\setminus i} w_{i,l,k} & i=l\\ 0 & \text{otherwise}\end{cases}, \tag{6}$$

with $d_{i,k}=|\mathrm{N}_{i,k}|$ the cardinality of $\mathrm{N}_{i,k}$. This choice is average preserving and for certain problems of distributed consensus, it provides asymptotic convergence to a global solution under mild conditions on the sequence of sets of active edges ε_k.

The consensus update phase is completely asynchronous. The i^{th} field sensor applies consensus if it is connected to a relay node at $k=k_i$. With the given network topology, the direct

communication between glider agents is not possible. However, sensors indirectly combine their estimates among each other through the relay nodes. In other words, the estimate at relay nodes allows the diffusion of the information through the network and the convergence of any local agent estimates to the global statistic. At the same time, the glider applies correction to the navigation heading according to the control law in the next section II.E. The next update (*i.e.* the next glider surfacing) is at $k_i+\Delta_i$ where Δ_i is a random variable with given a distribution.

E. Vehicle control

Following [2], the local sensor control is obtained by updating the next agent positions to minimize the average predicted covariance of the scalar field estimate. Using the coefficient covariance matrix from the KF, this quantity is given by:

$$J = \int_A \mathbf{\Psi}(\mathbf{r})\hat{\mathbf{C}}_{k|k-1}\mathbf{\Psi}^T(\mathbf{r})dA\,, \tag{7}$$

where the integration is over the area A of interest, in which the network of agents is constrained to operate. As in [2], the position $\mathbf{p}_{i,k}$ of the i^{th} agent is given by

$$\mathbf{p}_{i,k} = \mathbf{p}_{i,k-1} + \mathbf{f}_{i,k-1}\,, \tag{8}$$

where the control input $\mathbf{f}_{i,k-1}$ is implemented by a gradient control law as follows:

$$\mathbf{f}_{i,k-1} = -S\frac{\partial J}{\partial \mathbf{p}_{i,k-1}}\,, \tag{9}$$

where

$$\frac{\partial J}{\partial \mathbf{p}_{i,k-1}} = \int_A \mathbf{\Psi}(\mathbf{r})\frac{\partial \hat{\mathbf{C}}_{k|k-1}}{\partial \mathbf{p}_{i,k-1}}\mathbf{\Psi}^T(\mathbf{r})dA\,, \tag{10}$$

and S is a constant gain. According to [2], for linear models, the m^{th} component of the control input vector (with m=1, 2, 3 in the 3D case) is given by an expression involving the state covariance matrix, the measurement matrix and its gradient with respect to the agent position as follows:

$$f_{i,m} = 2SR_i^{-1}\int_A \mathbf{\Psi}(\mathbf{r})\hat{\mathbf{C}}\frac{\partial \mathbf{H}^T}{\partial p_{i,m}}(\mathbf{p}_i)\mathbf{H}(\mathbf{p}_i)\hat{\mathbf{C}}\mathbf{\Psi}^T(\mathbf{r})dA\,, \tag{11}$$

where $\mathbf{H}(\mathbf{p}_i) = \mathbf{\Psi}(\mathbf{p}_i)$ is the agent measurement matrix according to (3) and $R_i = \rho_i^2$. The time step index has been dropped for the sake of clarity.

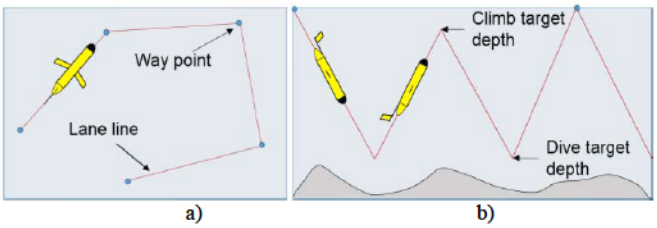

Fig. 4. Glider mission plan: a) way points and lane lines in the horizontal plane, and b) yo-yo trajectory in the vertical plane.

The dynamic of the agents in (8) is adapted, as specified below, to model the typical behavior of an underwater glider [17], having a constant speed (in absence of sea current), a constrained vertical plane dynamic and a waypoint guidance system. The wave glider is similarly modeled in 2D. Generally, an underwater glider moves through a 3D space following a saw-tooth shape trajectory (see Fig. 4) in the vertical plane. The trajectory is composed of a certain number of dive/climb cycles in the interval between two surfacing phases of the glider (during which data transmission is possible). The data, collected during each dive or climb cycle, are stored and finally transmitted during the surfacing phase.

The underwater glider dynamic model considered in this work assumes a constant velocity without water current disturbances, constrained to follow a yo-yo trajectory in the vertical plane with given climbing and diving target depths [18]. The glider navigates in the vertical plane along a yo-yo segment with a given constant pitch angle ϕ. The control vector (9) is normalized and multiplied by the total glider speed V to take into account the constant speed constraint:

$$\tilde{\mathbf{f}}_{i,k} = V\mathbf{f}_{i,k} / \| \mathbf{f}_{i,k} \|\,. \tag{12}$$

As the dynamic in the vertical plane is constrained as described above, the 2D version of the control law (8) on the horizontal plane is applied at each glider surfacing to optimally change the vehicle direction. For the wave glider the same control law is applied every time there is a connection with a RN.

III. Results

The test scenario is simulated by using 3D forecasts of sea water temperature of the NCOM forecast model [12]. The forecasts were provided by the Naval Research Laboratory-Stennis Space Centre (NRL–SSC), during the STO–CMRE 2011 Recognized Environmental Picture cruise trial (REP11) in the Mediterranean Sea. The scenario covers a time period of about 7 days (the total observation time is T_D=165 h), and a spatial domain of 60 by 60 Km in the horizontal plane and 100 m depth. The forecast interval is 3h. Fig. 5 shows a 3D example of the true field at the end of the considered observation period (excess variations with respect to the total average are displayed).

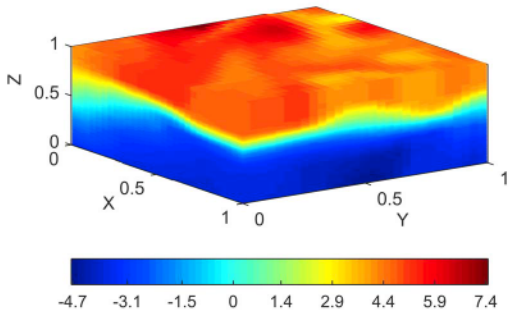

Fig. 5. NCOM water temperature excess field at the end of the simulation period. Temperature in °C.

The network simulation scenario reported here is composed of 9 underwater gliders and 3 wave gliders aided by

a surface network of 5 relay nodes distributed as in Fig. 6. In both Fig. 5 and Fig. 6, and in the sequel, the coordinates are normalized between 0 and 1 for convenience. The simulation is run for two different communication ranges of R_{tx}=10 and R_{tx}=20 km as depicted in Fig. 6 (the vehicles within the red circles can communicate with the RNs), with the second case providing the full coverage of the horizontal plane. It is supposed that a vehicle communicates with the closest RN within its transmission range. The underwater gliders have a constant pitch angle of 26° and a speed of 0.7 m/s. They emerge at surface for communicating with the RNs every 1.5 hours plus a random variable uniformly distributed between −20 and +20 minutes. The wave gliders have the same speed as the underwater ones and communicate with the RNs with the same cadence. The communications between underwater and wave gliders are not allowed. For both type of vehicles the guidance and navigation system is way point based. At each communication event, the control law (8) in 2D (for the horizontal plane) is applied to steer the connected vehicles toward the new way point. The RN network is fully connected and is triggered to apply consensus and diffuse new information among its nodes every time a connection with one or more vehicles is established.

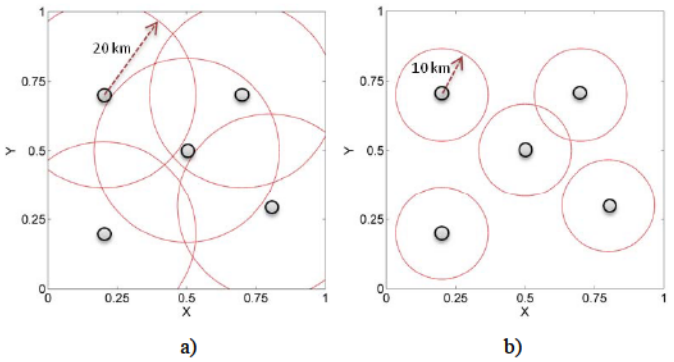

Fig. 6. RN network configuration with two different maximum communication ranges. a) R_{tx}=20 km, b) R_{tx}=10 km.

The spatial domain is discretized into a 30×30×30 3D regular grid resulting in a horizontal resolution of 2 km and a vertical resolution of 3.33 m. The sampling rate is T=6 s. The field is modeled using 512 3D Gaussian RBFs distributed on a regular 8×8×8 sub-grid of the main discretization grid. The RBF spreading parameter is β=0.025 constant for all the base functions and along the 3 spatial directions. The RBF spread parameter was chosen empirically by estimating the spatial scale of the main oceanographic features present in the data. The state equation (2) has a constant transition matrix $\mathbf{F}_k=\mathbf{I}_{512}$, where $\mathbf{I}_{512}$ is the 512×512 identity matrix. The process noise covariance matrix is set to $\mathbf{Q}_k=0.003\mathbf{I}_{512}$. The measurement equation of each agent is (3) with measurement noise variance equal to $\rho_{i,k}^2 = 0.001$. The simulation is initialized by setting the coefficient values to zero and the initial coefficient vector covariance to $\mathbf{C}_0=0.5\mathbf{I}_{512}$. The position of the vehicles on the horizontal plane is uniformly chosen at random.

Fig. 7 shows the variations of the field root mean square error (RMSE) for all the network nodes, within the 7 days observation period, for the two values of the communication range R_{tx}. For R_{tx}=10 km, the network does not reach a consensus as the RMSE of the nodes shows a higher dispersion and average value with respect to R_{tx}=20 km. The lack of communication coverage implies a low average network connectivity thus resulting in a low information exchange among the nodes and by consequence in a poor estimate and tracking of the dynamic of the field. The full coverage solution (R_{tx}=20 km) achieves consensus showing a lower RMSE dispersion and average value, and a better dynamic behavior and convergence.

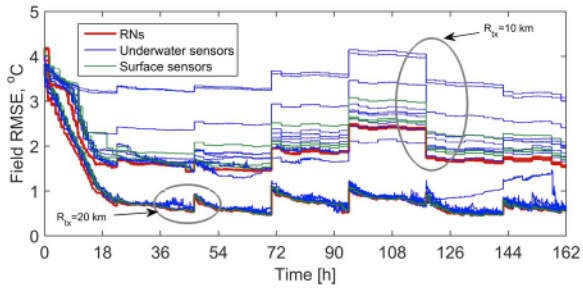

Fig. 7. Temporal graph of the RMSE of the excess field estimate for the RNs and the vehicles, and for R_{tx}=10 km and R_{tx}=20 km.

The test demonstrates that it is crucial to find the best tradeoff between network costs, in terms of number of network nodes and energy budget, and network estimation performance. Future work will be addressed to investigate if an optimal or sub-optimal tradeoff among the network parameters can be found. For the sake of clarity, the results reported below are for the case R_{tx}=20 km.

As an example, Fig. 8 shows the estimates of the maximum energy coefficient of the field RBF expansion for three different nodes of the network, an RN, an underwater sensor and a surface sensor. The three different estimates achieve consensus after transitory phases that are related to the field temporal variability.

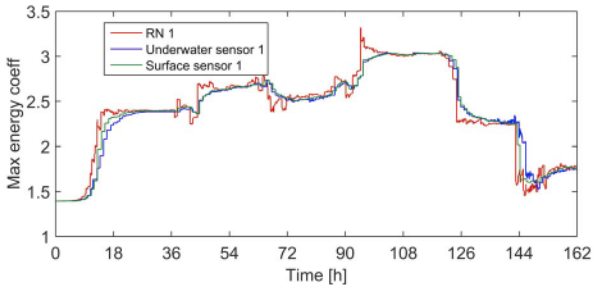

Fig. 8. Estimate of the maximum energy coefficient for different nodes of the network. R_{tx}=20 km.

Fig. 9 depicts the field estimate of the three surface sensors along the tracks of the first one (to assess the quality of an estimate in positions that are far from the positions where a sensor has collected measurements). The first sensor estimate, at the beginning of the observation period, is obviously closer to the true field with respect to the other sensors (see for

instance the initial value of sensor 3 estimate). After about 27 hours since the base time of the simulation, all the estimates reach a consensus and start to track the field variations more closely.

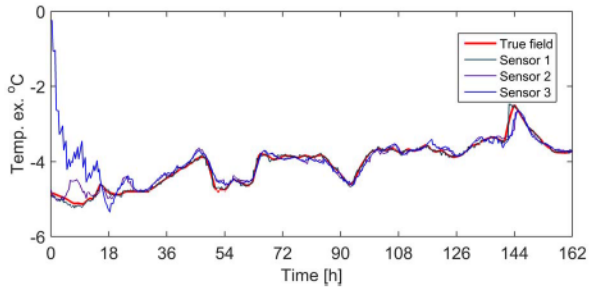

Fig. 9. Temperature excess field estimated by the surface sensors versus the true field for R_{tx}=20 km. The estimated fields are along the trajectory of the sensor 1.

Fig. 10-a shows the transitory phase in the first 3 hours of the simulation in which it is possible to see how the sensors progressively reach a consensus toward the true field. The true field and the estimates from the 9 sensors are plotted along the reference trajectory of the underwater sensor 1. Fig. 10-b shows the estimates and the true field along the same reference tracks during a regime phase between +100h and +103h since the simulation base time. Thanks to the information flowing from one sensor to the others through the RNs, the sensor estimates reach a consensus converging in average to the true temperature excess field.

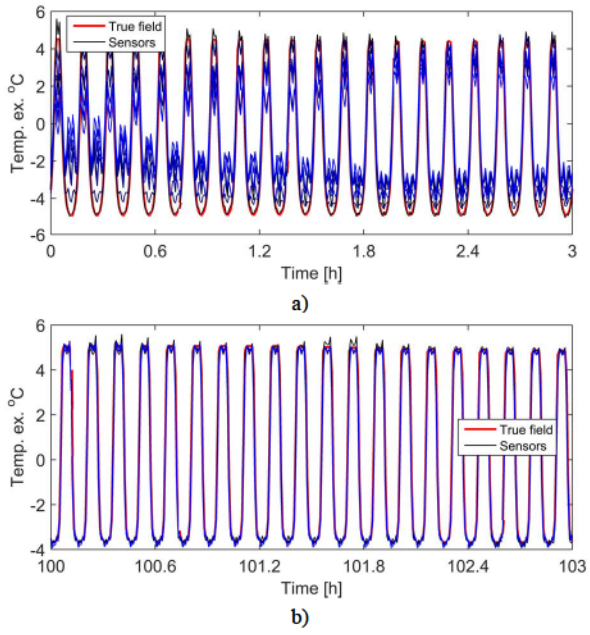

Fig. 10. Temperature field in the first 3 hours of simulation estimated by the underawater sensors, along the tracks of sensor 1. a) the picture shows the transitory phase in which all the sensors progressively reach consensus as in the regime phase depicted in b).

Fig. 11 provides a 3D view of the temperature excess field estimation of the RN 1 at the end of the observation period, showing a good agreement with the true field in Fig. 5 with the main water column structures well resolved.

Fig. 12 further confirms the good reconstruction of the main oceanographic features in the water column by displaying the excess temperature field in the vertical direction, within the observation period and along the trajectory of a reference underwater sensor.

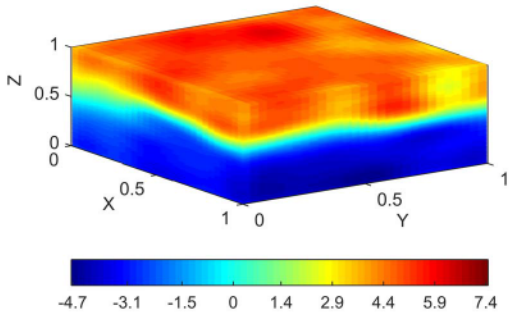

Fig. 11. Estimation of the 3D water temperature field at the end of the observation period for R_{tx}=20 km and RN 1. Temperature in °C.

In particular, Fig. 12-a shows the true field, Fig. 12-b the field estimate of the reference sensor and Fig. 12-c the field of the surface sensor. After a transitory phase, especially visible in the surface vehicle case, the estimates provide, in general, a good reconstruction of the basic water column features, such as the thermo-cline variability and some masses of warmer water toward the end of the observation interval.

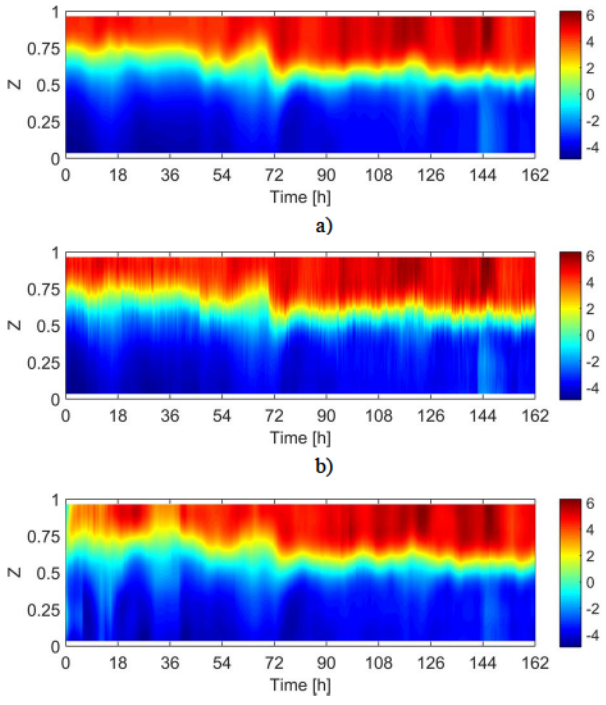

Fig. 12. True field and estimated field in the vertical direction along the trajectory of the underwater glider 1 for R_{tx}=20 km. a) true field, b) estimated field by sensor 1, c) estimated field by surface sensor 1. Temperature in °C.

IV. Conclusions

In this paper, we demonstrate the feasibility of a distributed field estimation algorithm based on a dynamic sensor network of underwater and surface agents complemented with a network of RNs. The architecture is based on agent local Kalman filter-based field estimation and asynchronous consensus to share field local statistics among agents and RNs. The control of the agents is based on local estimates updated by the consensus algorithm. This allows an agent to use global information to control its position in order to acquire field measurements in the most informative areas and adaptively track the field variations. The system achieves an estimate of the global field that is shared by all the nodes of the network.

The test case scenario here presented simulates a sensor network of 9 underwater gliders and 3 wave gliders with limited communication capabilities with a surface network of 5 RNs glider fleet mission of 7 days using 3D time-varying seawater temperature data provided by the NCOM forecast model for a Mediterranean Sea area, in the framework of the REP11 experiment. For typical fleet operational parameters (i.e. 12 agents and 1.5 hours surfacing and communication average period) and surveyed area size (60×60 Km horizontally and 100 m vertically) the average performance achieved in terms of RMSE at steady state is within 0.5 °C.

Future work will be addressed to investigate optimal network deployment methods in order to optimize the trade-off between network costs and estimation performance. Methods to reduce the communication overhead mainly due to the exchange of estimate covariance matrices will be also investigated. Furthermore, additional work is envisioned to investigate the effects on network performance of the water current affecting the agent navigation.

Acknowledgment

This work has been funded by the NATO Allied Command Transformation (NATO–ACT) under the projects SAC000405, SAC000510–Environmental Knowledge and Operational Effectiveness–Decisions in Uncertain Ocean Environments (EKOE–DUOE). NCOM forecasts are provided by the US Naval Research Laboratory–Stennis Space Center (NRL–SSC) in the framework of the STO–CMRE REP11 experiment.

References

[1] Alvarez, A.; Garau, B.; Caiti, A., "Combining networks of drifting profiling floats and gliders for adaptive sampling of the Ocean," Robotics and Automation, 2007 IEEE International Conference on , vol., no., pp.157,162, 10-14 April 2007, doi: 10.1109/ROBOT.2007.363780.

[2] K. M. Lynch et al, "Decentralized Environmental Modeling by Mobile Sensor Networks," Robotics, IEEE Transactions on, Vol. 24, No 3, June 2008.

[3] Sheng-Yuan Tu; Sayed, A.H., "Mobile Adaptive Networks," Selected Topics in Signal Processing, IEEE Journal of , vol.5, no.4, pp.649,664, Aug. 2011, doi: 10.1109/JSTSP.2011.2125943.

[4] Olfati-Saber, R.; Fax, J.A.; Murray, R.M., "Consensus and Cooperation in Networked Multi-Agent Systems," Proceedings of the IEEE , vol.95, no.1, pp.215,233, Jan. 2007, doi: 10.1109/JPROC.2006.887293

[5] P. Braca, S. Marano, and V. Matta, "Enforcing Consensus While Monitoring the Environment in Wireless Sensor Networks," Signal Processing, IEEE Transactions on, 2008.

[6] P. Braca, S. Marano, V. Matta and Ali H. Sayed, "Asymptotic Performance of Adaptive Distributed Detection over Networks," IEEE Transactions on Information Theory

[7] P. Braca, S. Marano, V. Matta and Ali H. Sayed, "Large Deviations Analysis of Adaptive Distributed Detection," Proc. of the IEEE International Conference on Acoustics, Speech, and Signal Processing (ICASSP 2014), Florence 2014.

[8] Hung Manh La; Weihua Sheng, "Distributed Sensor Fusion for Scalar Field Mapping Using Mobile Sensor Networks," IEEE Transactions on Cybernetics, vol.43, no.2, pp.766, 778, April 2013.

[9] R. Grasso, P. Braca, S. Fortunati, F. Gini, M. S. Greco, "Dynamic Underwater Glider Network for Environmental Field Estimation," IEEE Transaction on Aerospace and Electronic Systems, under review.

[10] R. Grasso, P. Braca, S. Fortunati, F. Gini, M. S. Greco, "Environmental Field Estimation by Consensus Based Dynamic Sensor Network and Underwater Gliders," 2015 European Signal Processing Conference (EUSIPCO 2015), under review.

[11] Tropp, J.A.; Laska, J.N.; Duarte, M.F.; Romberg, J.K.; Baraniuk, R.G., "Beyond Nyquist: Efficient Sampling of Sparse Bandlimited Signals," IEEE Transactions on Information Theory, vol.56, no.1, pp.520-544, Jan. 2010.

[12] Martin, P. J., "A description of the Navy Coastal Ocean Model Version 1.0," NRL Rep. NRL/FR/7322– 00–9962, 42 pp., NRL, Stennis Space Center, MS, USA, 2000.

[13] Julier, S., J., Uhlmann, J., K., "Unscented Filtering and Nonlinear Estimation," Proceedings of the IEEE, Vol. 92, No. 3, March 2004.

[14] Olfati-Saber, R.; Murray, R.M., "Consensus problems in networks of agents with switching topology and time-delays," IEEE Transactions on Automatic Control, vol.49, no.9, pp.1520-1533, Sept. 2004.

[15] P. Braca, S. Marano, V. Matta and P. Willett, "Consensus-Based Page's Test in Sensor Networks," Signal Processing, 2011.

[16] P. Braca, S. Marano, V. Matta and P. Willett, "Asymptotic Optimality of Running Consensus in Testing Binary Hypotheses," IEEE Transactions on Signal Processing, 2010.

[17] Schofield, O., J. Kohut, D. Aragon, L. Creed, J. Graver, C. Haldeman, J. Kerfoot, H. Roarty, C. Jones, D. Webb, and S.M. Glenn., "Slocum gliders: Robust and ready," Journal of Field Robotics 24(6):1–14, 2007.

[18] Grasso R, Cecchi D, Cococcioni M, Trees C, Rixen M, Alvarez A, Strode C, "Model based decision support for underwater glider operation monitoring," Proceedings OCEANS 2010 MTS/IEEE, Seattle. pp. 1–8, 2010.

Document Data Sheet

Security Classification		Project No.
Document Serial No.	**Date of Issue**	**Total Pages**
CMRE-PR-2019-128	June 2019	7 pp.

Author(s)

Raffaele Grasso, Paolo Braca, Stefano Fortunati, Fulvio Gini, Maria S. Greco

Title

Distributed underwater glider network with consensus Kalman filter for environmental field estimation

Abstract

A distributed coordinated dynamic sensor network for optimal environmental field estimation is proposed and tested on simulated and real data. The architecture is used to distribute the estimation of 3D time-varying fields on a network of underwater gliders in which communication constraints are one of the main limiting factors for achieving complete network automation and de-centralization. The dynamic network is integrated with a network of relay nodes that the agents can reach at the surface through satellite or radio links. Local field statistics are estimated by a Kalman filter-based algorithm by agents and the information in the network is shared by using the asynchronous consensus algorithm. The system is tested on realistic scenarios that are simulated by true oceanographic forecast models. A heterogeneous network of underwater and surface wave gliders is used to estimate 3D sea water temperature fields. Simulation results show that the network achieves a consensus with an average root mean square error at steady state that is below 0.5 °C.

Keywords

Autonomous vehicles, distributed processing, sensor networks, consensus, optimal field estimation.

Issuing Organization

NATO Science and Technology Organization
Centre for Maritime Research and Experimentation

Viale San Bartolomeo 400, 19126 La Spezia, Italy

[From N. America:
STO CMRE
Unit 31318, Box 19, APO AE 09613-1318]

Tel: +39 0187 527 361
Fax:+39 0187 527 700

E-mail: library@cmre.nato.int